Electronic excitation of CH4 by low-energy electron impact

Carl Winstead, Qiyan Sun, Vincent McKoy, José L. S. Lino, and Marco A. P. Lima

Citation: The Journal of Chemical Physics **98**, 2132 (1993); doi: 10.1063/1.464191
View online: http://dx.doi.org/10.1063/1.464191
View Table of Contents: http://scitation.aip.org/content/aip/journal/jcp/98/3?ver=pdfcov
Published by the AIP Publishing

Articles you may be interested in

Raman scattering of light by low-energy electronic excitations of the Tb 3 + ion in the crystal KTb (WO 4) 2
Low Temp. Phys. **33**, 915 (2007); 10.1063/1.2747049

Electronic excitation of silane (SiH4) by low-energy electron impact
J. Chem. Phys. **101**, 338 (1994); 10.1063/1.468492

Low-energy electron impact study of acetone
J. Chem. Phys. **61**, 763 (1974); 10.1063/1.1682015

Angular Dependence of Low-Energy Electron-Impact Excitation Cross Section of the Lowest Triplet States of H2
J. Chem. Phys. **49**, 5464 (1968); 10.1063/1.1670073

Differences in the Angular Dependencies of Spin- and Symmetry-Forbidden Excitation Cross Sections by Low-Energy Electron Impact Spectroscopy
J. Chem. Phys. **48**, 945 (1968); 10.1063/1.1668744

AIP | APL Photonics

APL Photonics is pleased to announce Benjamin Eggleton as its Editor-in-Chief

This article is copyrighted as indicated in the article. Reuse of AIP content is subject to the terms at: http://scitation.aip.org/termsconditions. Downloaded to IP: 131.215.248.200 On: Sat, 17 Oct 2015 05:29:25

Electronic excitation of CH_4 by low-energy electron impact

Carl Winstead, Qiyan Sun,[a] and Vincent McKoy
A. A. Noyes Laboratory of Chemical Physics,[b] California Institute of Technology, Pasadena, California 91125

José L. S. Lino
Instituto Técnológico da Aeronautica, Centro Técnico Aeroespacial, 12200 São José dos Campos, S. P., Brazil

Marco A. P. Lima
Instituto de Física "Gleb Wataghin"—Departamento de Electrônica Quântica, Universidade Estadual de Campinas, 13081 Campinas, S. P., Brazil

(Received 27 August 1992; accepted 23 October 1992)

We report cross sections for excitation of the $(1t_2 \rightarrow 3sa_1)$ singlet and triplet states of methane by low-energy electron impact. The cross sections for these dissociative states were obtained using the Schwinger multichannel variational method with up to seven channels (three physical states) coupled. Aspects of the convergence with respect to channel coupling are discussed. A preliminary comparison with the recently measured CH_2 fragment production cross section [T. Nakano, H. Toyoda, and H. Sugai, Jpn. J. Appl. Phys. **30**, 2912 (1991)] shows fair agreement.

I. INTRODUCTION

Although low-energy electron-molecule collisions are of both fundamental and practical[1] interest, there is as yet little quantitative information on the electronically inelastic cross sections, especially for polyatomic molecules. In part this situation reflects the difficulty of the relevant experiments, and in part the absence, until recently, of adequate theoretical methods. In the past few years, however, there has been progress in computational approaches, and results have appeared for polyatomic molecules including water,[2] formaldehyde,[3,4] and ethylene.[5,6] In the present paper, we consider excitation of methane (CH_4) to its two lowest-lying excited states, the $(1t_2 \rightarrow 3sa_1)$ $^{1,3}T_2$ states. In a previous study[7] we have calculated cross sections for these states in a two-channel approximation; in this work we consider more extensive coupling schemes that include interactions among excited-state channels.

A study of these transitions is interesting for a number of reasons. Like all electronically excited states of methane,[8] the $(1t_2 \rightarrow 3sa_1)$ $^{1,3}T_2$ are dissociative. Since they have the lowest thresholds, the $1\,^3T_2$ and $1\,^1T_2$ states can be expected to play a large role in the production of reactive fragments within low-temperature plasmas used, for example, in the plasma-assisted chemical vapor deposition of diamond-like films.[9] On the theoretical side, there are as yet few *ab initio* studies of Rydberg-type excitations in molecules, and it is of interest to learn how such calculations compare to studies of valence excitations. Further, a theoretical prediction of dissociation cross sections for molecules such as methane will require the calculation of a number of discrete transitions, as well as procedures for extrapolation and for inclusion of the ionization continuum. Before undertaking such an ambitious program, it is useful to examine convergence with respect to basis set size and channel coupling within a more limited context.

The low-lying excited electronic states of methane have been the subject of numerous experimental and theoretical studies, although most previous work has emphasized the optically allowed singlet excitations. High energy, near-forward electron scattering experiments[10,11] place the singlet threshold at 8.55 eV, in good agreement with the threshold of 8.52 eV determined from photoabsorption measurements.[12] Assignment of a definite threshold energy is complicated, however, because the state is dissociative and in vertical transitions is accessed far from any local minima. For example, the electron-impact excitation experiments show maxima at 9.65 and 10.33 eV that have been interpreted[10,11] as components of the $^1T_2$ state that are split by Jahn–Teller distortion. In a low energy electron scattering experiment using the trapped electron method, Brongersma and Oosterhoff[13] placed the first triplet peak at 8.8 eV; however, the triplet threshold is certainly somewhat lower than this maximum. Theoretical determinations[14,15] of the *vertical* excitation energies have placed the $1\,^3T_2$ threshold at 9.96 and 9.97 eV, while theoretical values for the $1\,^1T_2$ vertical excitation energy include 10.4,[14] 10.24,[15] and 11.21 eV.[16] None of these calculations is extensive by current standards, and the large discrepancies among them are not surprising.

Theoretical studies[16–18] and photodissociation experiments[19] show that the lowest singlet state dissociates primarily to CH_2 and H_2. According to the calculations, dissociation leads to $1\,^1B_1$ methylene and $X\,^1\Sigma_g^+$ hydrogen. Similar calculations have apparently not been done for the $1\,^3T_2$ state of methane, but it seems plausible that it dissociates in similar fashion, i.e., to $X\,^3B_1$ CH_2 and $X\,^1\Sigma_g^+$ H_2. Emission cross sections for various fragments produced by electron impact or photofragmentation of CH_4 have been extensively studied.[20] Lyman-α emission appears at about 21 eV excitation energy, although energetically allowed

[a]Present address: Biosym Technologies, 9685 Scranton Road, San Diego, California 92121.
[b]Contribution No. 8709.

 0021-9606/93/032132-06$06.00 © 1993 American Institute of Physics

This article is copyrighted as indicated in the article. Reuse of AIP content is subject to the terms at: http://scitation.aip.org/termsconditions. Downloaded to IP: 131.215.248.200 On: Sat, 17 Oct 2015 05:29:25

above 14.7 eV. The absence of VUV emissions at lower excitation energies suggests that dissociation below 21 eV primarily leads to ground or metastable states of the neutral fragments and ions.

Recommended cross section data for various elastic and inelastic processes in CH_4 have recently been assembled by several authors.[21–23] We are not aware of any measured cross sections for excitation of the $(1t_2 \rightarrow 3sa_1)$ $^{1,3}T_2$ states by low-energy electrons. However, Vuškovič and Trajmar[24] have reported differential and integral cross sections for excitation of methane that do not resolve individual channels but rather sum over all channels whose thresholds lie within certain energy ranges. Nakano *et al.*[25] have recently measured cross sections for production of CH_2 and CH_3 fragments by electron impact. Since, as discussed above, the $(1t_2 \rightarrow 3sa_1)$ $^1T_2$ state and presumably the $^3T_2$ state dissociate primarily to CH_2, it is useful to compare our summed singlet and triplet cross sections with their CH_2 cross section, which should form an upper bound.

In the next section, we review the theory and the computational method used in the present study. Section III contains our results, and a discussion and concluding remarks are given in Sec. IV.

II. CALCULATIONS

These calculations employed the Schwinger multichannel (SMC) method, a variational procedure that has been described elsewhere.[26–28] We have recently implemented this procedure on distributed-memory parallel computers in order to address larger scattering problems in a cost-effective manner.[29,30] Most of the present work was done on the Intel iPSC/860 and Touchstone Delta computers of the Concurrent Supercomputing Consortium, although the Mark III^{fp} hypercubes of the Caltech Concurrent Supercomputing Facility were used for some smaller calculations.

In our implementation of the SMC method, the scattering wave function is represented entirely within an L^2 basis of spin-adapted configurations of molecular orbitals expanded in Cartesian Gaussian functions. Several Cartesian Gaussian basis sets were considered in the present work in order to gauge convergence. These basis sets ranged in size from 61 to 91 contracted functions. As in our earlier study,[7] we used a basis of 61 contracted Gaussians to describe the target states. This basis was obtained by adding two *s* functions (exponents 0.046 and 0.023), one *p* function (exponent 0.046), and three *d* functions (exponents 3.2, 0.8, and 0.2) to Dunning's[31] 5*s*3*p* C basis and one *p* Gaussian (exponent 1.0) to Dunning's 3*s* H basis. In addition to the virtual orbitals from this target basis, we included six *s* Gaussians (exponents 2.0, 1.0, 0.25, 0.08, 0.01, and 0.005), four *p* Gaussians (exponents 0.72, 0.2, 0.02, and 0.01), and two *d* Gaussians (exponents 1.6 and 0.4) to aid in representing the scattering orbitals in the two- and three-channel calculations described below. The additional Gaussians were Schmidt-orthogonalized to the occupied and virtual target orbitals. The same basis was used for the seven-channel calculations, except that the six additional *s* Gaussians were omitted; at the two- and three-channel level these functions had little effect on the cross sections. Both supplemental Gaussian sets are supersets of that used in Ref. 7.

The ground state of the CH_4 target was obtained from an SCF calculation and the excited states obtained using the improved virtual orbital (IVO) method[32] at the ground-state equilibrium geometry. The $^3T_2$ t_2 IVO was used for both the triplet and the singlet channels. The thresholds obtained in this manner are 10.86 eV for the $^3T_2$ state and 11.24 eV for the $^1T_2$ state, and the $^1T_2$ oscillator strength is 0.5065. For comparison, Williams and Poppinger[15] obtained energies of 9.97 and 10.24 eV for the $^3T_2$ and $^1T_2$ states and a $^1T_2$ oscillator strength of 0.393 from an equations-of-motion calculation. However, in a single-excitation CI calculation, which is more nearly comparable to our IVO calculation, the same authors obtained 10.55 and 10.96 eV, respectively, for the $^3T_2$ and $^1T_2$ thresholds and 0.572 for the $^1T_2$ oscillator strength, in closer agreement with our IVO results. Experimentally, the $^3T_2$ state is placed at 8.8 eV (Ref. 13) and the $^1T_2$ state at 9.65 eV,[10,11] although, as discussed in Sec. I, these values do not necessarily represent vertical excitation energies. The integrated oscillator strength density for 8.55–10.95 eV excitations is measured[11] to be 0.277, but how much of this is ascribable to the $^1T_2$ state and how much $^1T_2$ oscillator strength density lies above 10.95 eV are not known.

We examined three channel coupling schemes in the course of the present work. In the simplest approximation, as in our previous study,[7] we included only the ground state and one of the three degenerate $^3T_2$ or $^1T_2$ components, for a two-channel calculation. We also conducted three-channel studies in which both the triplet and the singlet spin states were included for a given T_2 component. Finally, we included all three components of both the $^3T_2$ and the $^1T_2$ states, together with the ground state, in seven-channel calculations. Results obtained from these three coupling schemes will be compared below.

Numerical stability proved to be a critical issue in these studies. Previously described techniques[4,33] were employed to obtain stable solutions to the linear equations associated with the SMC variational principle. Agreement among results in several different basis sets leads us to believe that the cross sections reported below are well converged.

Since the transition to the $^1T_2$ state is allowed by the electric dipole selection rule, it exhibits strong near-forward (large impact parameter) scattering.[34] A sensible procedure for including this effect in fixed-nuclei calculations,[6,35] which we have employed here, is to obtain the low partial wave components of the scattering amplitude from a high-order theory such as the SMC method, while including the high partial wave contribution in the Born approximation.[36,37] The two methods should give similar results at intermediate partial waves, so that the final results is more or less independent of the cutoff used for the SMC amplitude. In the present instance, we truncated the SMC contribution at $l=5$, $m=3$. Near $l=5$, the cross section was insensitive to changing the l cutoff; there was

This article is copyrighted as indicated in the article. Reuse of AIP content is subject to the terms at: http://scitation.aip.org/termsconditions. Downloaded to IP: 131.215.248.200 On: Sat, 17 Oct 2015 05:29:25

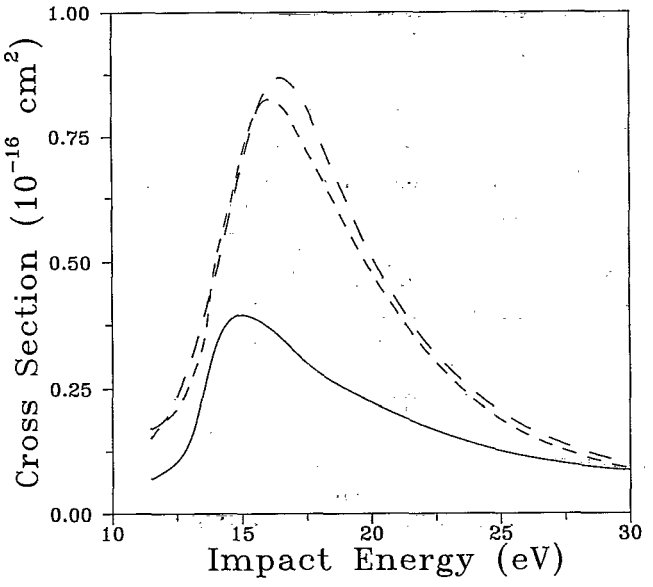

FIG. 1. Integral cross section for electron-impact excitation of the $(1t_2 \rightarrow 3sa_1)$ $1\,^3T_2$ transition in methane. Long dash: two-channel calculation; short dash: three-channel calculation; solid line: seven-channel calculation.

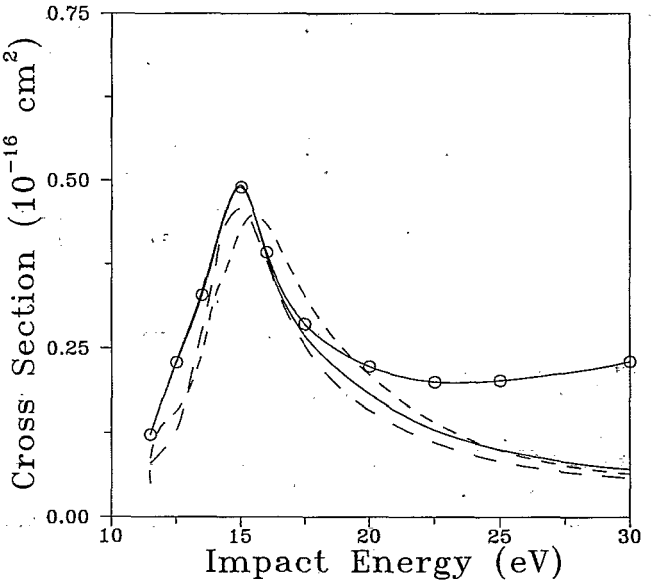

FIG. 2. As in Fig. 1, for the $(1t_2 \rightarrow 3sa_1)$ $1\,^1T_2$ transition, except that seven-channel results including the Born correction are shown (solid line with circles).

more sensitivity to the m cutoff, but we believe much of this sensitivity derives from the inability of the basis set we used to represent well contributions from $m=4$ and higher. Those contributions should, however, be well represented in the Born approximation.

III. RESULTS

Integral cross sections for the $(1t_2 \rightarrow 3sa_1)$ $^3T_2$ and $^1T_2$ excitations are presented in Figs. 1 and 2, respectively. For comparison, each figure contains the results of several different calculations. In Fig. 1, we show two-, three-, and seven-channel cross sections for the $^3T_2$ excitation. Figure 2 is similar but also includes Born-corrected $^1T_2$ values for the seven-channel calculation.

A few interesting points may be noted immediately. Comparison of the two- and three-channel results shows that the inclusion of singlet-triplet excited-state coupling does not have a dramatic effect, the only large change being in the tail of the $^1T_2$ peak. On the other hand, including coupling among all the degenerate $^3T_2$ and $^1T_2$ components greatly decreases the magnitude of the $^3T_2$ cross section except at 30 eV. No such qualitative effect is seen for the $^1T_2$ integral cross section, although, as described below, there are significant changes in the $^1T_2$ differential cross section.

The effect of including high partial wave scattering, through the Born-correction procedure, for the dipole-allowed $(1t_2 \rightarrow 3sa_1)$ $^1T_2$ transition is seen in Fig. 2 to be quite small below 20 eV, reflecting both the suppression of the Born-dipole scattering by its $\log[(k+k')/|(k-k')|]$ dependence near threshold $(k' \rightarrow 0)$ and also the strength of short-range, low-partial-wave interactions at low energy. At higher energies, however, the uncorrected $^1T_2$ cross section drops off rapidly, while the dipole contribution becomes quite substantial. Indeed, most of the $^1T_2$ cross section at 30 eV is due to the dipole component.

Differential cross sections at selected energies are shown in Figs. 3 and 4 for the $^3T_2$ and $^1T_2$ states, respectively. As for the integral cross sections of Figs. 1 and 2, two-, three-, and seven-channel results are shown, including Born-corrected seven-channel results in Fig. 4. Look-

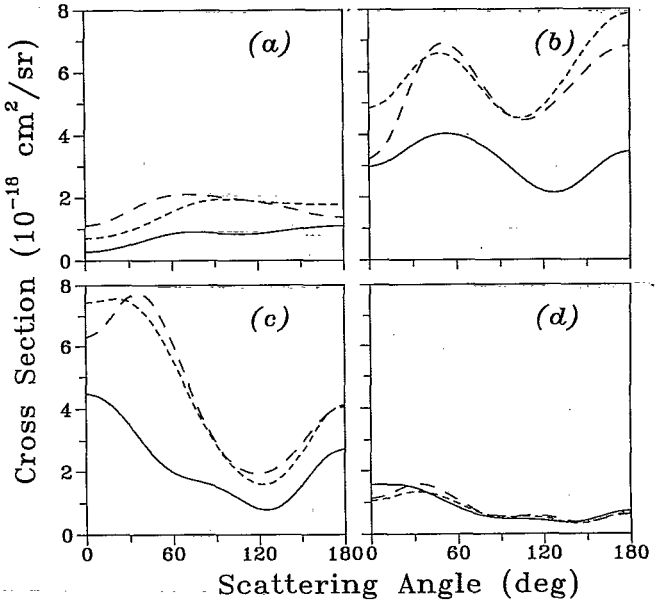

FIG. 3. Differential cross sections for the $1\,^3T_2$ excitation of methane, at (a) 12.5 eV, (b) 15 eV, (c) 20 eV, and (d) 30 eV impact energy. Long dash: two-channel calculation; short dash: three-channel calculation; solid line: seven-channel calculation.

This article is copyrighted as indicated in the article. Reuse of AIP content is subject to the terms at: http://scitation.aip.org/termsconditions. Downloaded to IP: 131.215.248.200 On: Sat, 17 Oct 2015 05:29:25

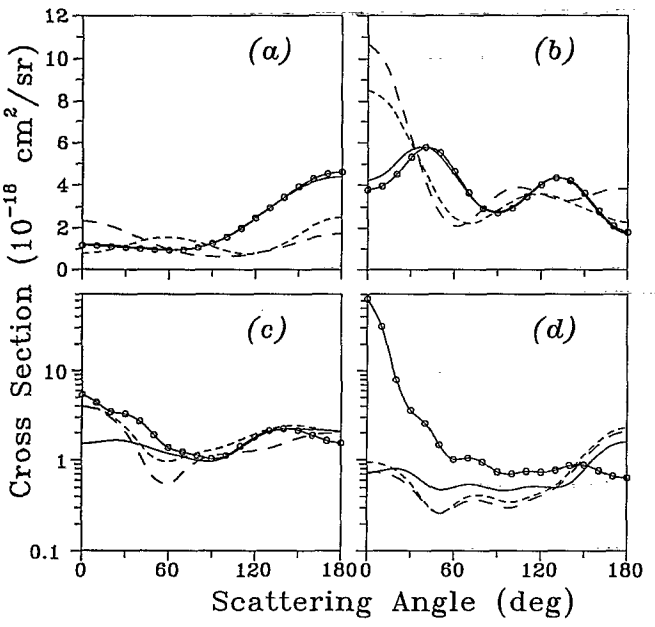

FIG. 4. As in Fig. 3 for the 1 $^1T_2$ excitation, except that seven-channel results including the Born correction are shown (solid line with circles).

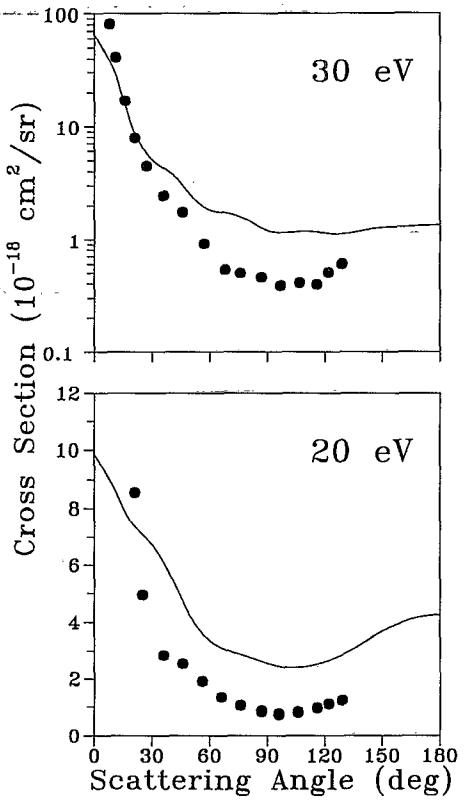

FIG. 5. Differential cross sections for electron-impact excitation of methane. Solid lines: summed 1 $^3T_2$ and 1 $^1T_2$ seven-channel cross sections; circles: summed measurements of Ref. 24 for energy losses of 7.5 to 10.5 eV.

ing first at the $^3T_2$ transition, Fig. 3, we see that the seven-channel cross section, though reduced in magnitude, is qualitatively similar to the two- and three-channel cross sections. The scattering is fairly isotropic near threshold and becomes forward peaked at higher energy [Figs. 3(c) and 3(d)]. The latter behavior is somewhat unusual, since backward-peaked differential cross sections are normally associated with singlet-to-triplet excitation at these energies. At 15 eV, near the maximum in the integral cross section, the differential cross section has an undulatory form, with a maximum and a minimum at intermediate angles. For the seven-channel calculation, these fall at about 50° and 130°, respectively. This behavior may reflect the contribution of a resonant scattering mechanism; however, the width of the peak in the $^3T_2$ cross section suggests that any core-excited shape resonance that might exist is short-lived.

Whereas the seven-channel $^3T_2$ differential cross section was qualitatively similar to the two- and three-channel results, though different in magnitude, the seven-channel $^1T_2$ differential cross section, Fig. 4, though of comparable magnitude, differs qualitatively from the singlet cross sections obtained in the two- and three-channel calculations. In fact, a comparison of Figs. 3 and 4 shows that in the seven-channel calculation, the $^1T_2$ differential cross section (before the Born-dipole correction is added) has become quite similar to that of the $^3T_2$ excitation.

In Fig. 5, we compare our summed $^1T_2$ and $^3T_2$ differential cross sections at 20 and 30 eV with the differential cross sections measured by Vušković and Trajmar.[24] For the purposes of this comparison we have summed the latter results for energy losses of 7.5–9 and 9–10.5 eV. The latter range may include contributions from higher-lying electronic states, and conversely, the 1 $^3T_2$ and 1 $^1T_2$ state may contribute to scattering at higher energy losses than 10.5 eV. As seen from the figure, the shapes of the experimental and theoretical cross sections are similar at intermediate angles, but the theoretical result is larger in magnitude. The disagreement at small angles may be ascribed to the contribution of other dipole-allowed excitations to the measurement.

In Fig. 6, we show our summed $^1T_2$ and $^3T_2$ integral cross sections along with the measured CH_2 production cross section of Nakano *et al.*[25] Also shown are the integral excitation cross sections at 20 and 30 eV for 7.5–10.5 eV energy loss.[24] As in Fig. 5, some caution is necessary in making the comparisons. Although, as noted earlier, CH_2 is probably the primary dissociation product of $(1t_2 \rightarrow 3sa_1)$ $^{1,3}T_2$ excitation, some CH_3 may also be produced, and of course other processes than $(1t_2 \rightarrow 3sa_1)$ excitation will lead to CH_2 production. Assuming dissociation of the $(1t_2 \rightarrow 3sa_1)$ $^{1,3}T_2$ states to CH_3 is negligible, the CH_2 cross section should form an upper bound to the $(1t_2 \rightarrow 3sa_1)$ cross section. As seen in Fig. 6, our cross section and the CH_2 cross section are of comparable magnitude, and the $(1t_2 \rightarrow 3sa_1)$ $^{1,3}T_2$ cross section does lie below the CH_2 cross section at most energies, though the peak near 15 eV appears to be too high. Our $^{1,3}T_2$ cross section and the CH_2 cross section are both much larger than the 7.5–10.5 eV energy loss integral cross section at 20 eV, but are in fair agreement with it at 30 eV.

This article is copyrighted as indicated in the article. Reuse of AIP content is subject to the terms at: http://scitation.aip.org/termsconditions. Downloaded to IP: 131.215.248.200 On: Sat, 17 Oct 2015 05:29:25

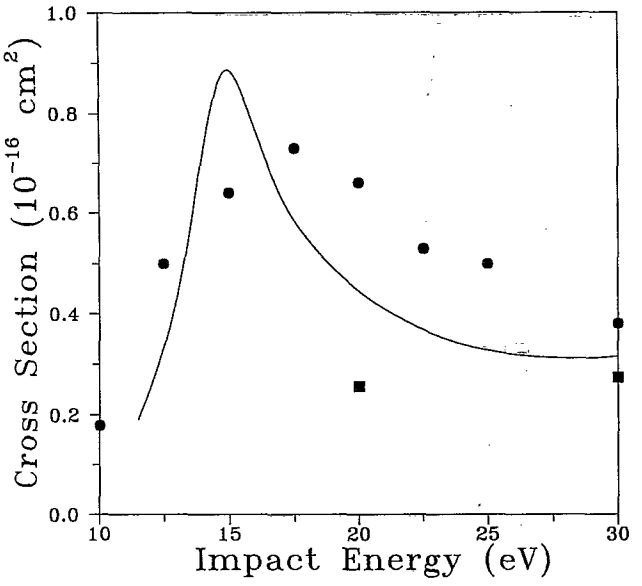

FIG. 6. Integral inelastic cross sections for methane. Solid line: summed $1\,^3T_2$ and $1\,^1T_2$ seven-channel cross sections; squares: summed measurements of Ref. 24 for energy losses of 7.5 to 10.5 eV; circles: CH_2 production cross section, Ref. 25.

IV. DISCUSSION AND CONCLUSION

As discussed earlier, several factors complicate the study of electron impact excitation cross sections in methane. Among these are the dissociative character of the excited states, the close spacing of thresholds, and the fact that vertical excitations reach strongly repulsive parts of the upper potential energy surfaces. It is therefore difficult to determine the origin of observed differences between theoretical results and the limited experimental data available. However, a few general observations can be made. First of all, the large changes in the triplet integral cross section and in the singlet differential cross sections on going from two- or three-channel coupling to seven-channel coupling suggest that further studies, in which still more elaborate coupling schemes are employed, will be necessary before we can be confident that convergence with respect to channel coupling has been achieved. In particular, it would be useful to look at the effect on the $(1t_2 \rightarrow 3sa_1)$ $^{1,3}T_2$ cross sections of including $(1t_2 \rightarrow 3pt_2)$ channels in the calculation, since the thresholds for the various channels arising from this configuration are nearby. These states are of course interesting in their own right and might be expected to make large contributions to the neutral dissociation cross sections.

Other limitations of the present calculations may also affect the comparison with experiment. Most obviously, it would be helpful to study the excitation process as a function of nuclear geometry, since the excited state character changes rapidly as the nuclei move toward dissociation.[16–18] It should also be mentioned that the dipole scattering contribution to the singlet cross section is sensitive to the oscillator strength of the excitation. Since the oscillator strength we obtain seems rather high in comparison to more elaborate calculations[15] and to experiment,[10] a better representation of the singlet excited state might be expected to lead to some reduction in the cross section.

In spite of the limitations noted above, the present calculation is useful in elucidating the potential sensitivity of the cross sections for these Rydberg excitations to coupling among excited states, and does in fact provide a reasonable estimate of the CH_2 fragment cross section. Such estimates may be useful for other molecular systems in which experimental data are lacking.

ACKNOWLEDGMENTS

This work made use of the Mark III^{fp} computers of the Caltech Concurrent Supercomputing Facility and of the Intel iPSC/860 and Touchstone Delta Computers of the Concurrent Supercomputing Consortium. Financial support by the National Science Foundation under Grant No. PHY-9021933 and by the Strategic Defense Initiative Organization through the Army Research Office is gratefully acknowledged.

[1] Japan Technical Information Service, *Plasma Reactions and Their Applications* (ASM International, Metals Park, Ohio, 1988).
[2] H. P. Pritchard, V. McKoy, and M. A. P. Lima, Phys. Rev. A **41**, 546 (1990).
[3] T. N. Rescigno, B. H. Lengsfield III, and C. W. McCurdy, Phys. Rev. A **41**, 2462 (1990).
[4] Q. Sun, C. Winstead, V. McKoy, J. S. E. Germano, and M. A. P. Lima, Phys. Rev. A **46**, 2462 (1992).
[5] Q. Sun, C. Winstead, V. McKoy, and M. A. P. Lima, J. Chem. Phys. **96**, 3531 (1992).
[6] T. N. Rescigno and B. I. Schneider, Phys. Rev. A **45**, 2894 (1992).
[7] C. Winstead, Q. Sun, V. McKoy, J. L. S. Lino, and M. A. P. Lima, Z. Phys. D **24**, 141 (1992).
[8] G. Herzberg, *Molecular Spectra and Molecular Structure III. Electronic Spectra of Polyatomic Molecules* (Van Nostrand Reinhold, New York, 1966), p. 527.
[9] See, for example, Y. H. Shing, F. S. Pool, and D. H. Rich, Thin Solid Films **212**, 150 (1992), and references therein.
[10] W. R. Harshbarger and E. N. Lassettre, J. Chem. Phys. **58**, 1505 (1972).
[11] M. A. Dillon, R.-G. Wang, and D. Spence, J. Chem. Phys. **80**, 5581 (1984).
[12] Ref. 8, p. 619.
[13] H. H. Brongersma and L. J. Oosterhoff, Chem. Phys. Lett. **3**, 437 (1969).
[14] F. Pauzat, J. Ridard, and B. Levy, Mol. Phys. **23**, 1163 (1972).
[15] G. R. J. Williams and D. Poppinger, Mol. Phys. **30**, 1005 (1975).
[16] M. S. Gordon and J. W. Caldwell, J. Chem. Phys. **70**, 5503 (1979).
[17] M. S. Gordon, Chem. Phys. Lett. **44**, 507 (1976).
[18] M. S. Gordon, Chem. Phys. Lett. **52**, 161 (1977).
[19] J. R. McNesby and H. Okabe, Advan. Photochem. **3**, 157 (1964), and references cited therein.
[20] K. D. Pang, J. M. Ajello, B. Franklin, and D. E. Shemansky, J. Chem. Phys. **86**, 2750 (1987), and references cited therein.
[21] D. K. Davies, L. E. Kline, and W. E. Bies, J. Appl. Phys. **65**, 3311 (1989).
[22] W. L. Morgan, JILA Data Center Rept. No. 34 (Joint Institute for Laboratory Astrophysics, Boulder, 1991).
[23] I Kanik, S. Trajmar, and J. C. Nickel, J. Geophys. Res. (in press).
[24] L. Vušković and S. Trajmar, J. Chem. Phys. **78**, 4947 (1983).
[25] T. Nakano, H. Toyoda, and H. Sugai, Jap. J. Appl. Phys. **30**, 2908 (1991); **30**, 2912 (1991).
[26] K. Takatsuka and V. McKoy, Phys. Rev. A **24**, 2473 (1981).
[27] K. Takatsuka and V. McKoy, Phys. Rev. A **30**, 1734 (1984).
[28] M. A. P. Lima, L. M. Brescansin, A. J. R. da Silva, C. Winstead, and V. McKoy, Phys. Rev. A **41**, 327 (1990).
[29] P. G. Hipes, C. Winstead, M. A. P. Lima, and V. McKoy, *Proceedings*

This article is copyrighted as indicated in the article. Reuse of AIP content is subject to the terms at: http://scitation.aip.org/termsconditions. Downloaded to IP: 131.215.248.200 On: Sat, 17 Oct 2015 05:29:25

of the Fifth Distributed Memory Computing Conference, Volume I: Applications, edited by D. W. Walker and Q. F. Stout (IEEE Computer Society, Los Alamitos, California, 1990), p. 498.
[30]C. Winstead, P. G. Hipes, M. A. P. Lima, and V. McKoy, J. Chem. Phys. **94**, 5455 (1991).
[31]T. H. Dunning, J. Chem. Phys. **53**, 2823 (1970).
[32]W. A. Goddard and W. J. Hunt, Chem. Phys. Lett. **24**, 464 (1974).
[33]C. Winstead and V. McKoy, Phys. Rev. A **41**, 49 (1990).
[34]M. J. Seaton, Proc. Phys. Soc. (London) **79**, 1105 (1962).
[35]L. A. Collins and D. W. Norcross, Phys. Rev. A **18**, 467 (1978).
[36]O. H. Crawford, A. Dalgarno, and P. B. Hays, Mol. Phys. **13**, 181 (1967).
[37]Q. Sun, C. Winstead, and V. McKoy, Phys. Rev. A **46**, 6987 (1992).

This article is copyrighted as indicated in the article. Reuse of AIP content is subject to the terms at: http://scitation.aip.org/termsconditions. Downloaded to IP: 131.215.248.200 On: Sat, 17 Oct 2015 05:29:25